

Particle velocities and long-range transport in classically forbidden regions

Jan Klaers,* Violetta Sharoglazova, and Chris Toebes
*Adaptive Quantum Optics (AQO), MESA⁺ Institute of Nanotechnology,
 University of Twente, 7522 NB Enschede, Netherlands*

We study the motion of massive particles in a system of two coupled waveguide potentials, where the population transfer between the waveguides effectively acts as a clock and allows particle velocities to be determined. Application of this scheme to tunneling phenomena at a reflective step potential reveals an energy-velocity relationship for classically forbidden motion and predicts the existence of classically forbidden long-range particle transport. Our work suggests that density gradients in wave functions are indicative of a genuine quantum mechanical type of motion.

Quantum mechanics knows a variety of velocity definitions, such as phase velocity, group velocity, velocities derived from the probability density flow or simply from the momentum operator. Particle velocities play a decisive role in the phenomenon of superfluidity [1–3], for example. For a superfluid described by the wave function $\psi(\mathbf{x}, t) = \sqrt{n(\mathbf{x}, t)} \exp(iS(\mathbf{x}, t))$, where $n(\mathbf{x}, t)$ denotes the density and $S(\mathbf{x}, t)$ the phase, the superfluid velocity is defined by

$$\mathbf{v}_s(\mathbf{x}, t) = \frac{\hbar}{m} \nabla S(\mathbf{x}, t). \quad (1)$$

This expression ascribes the velocity exclusively to phase gradients – but not to density or amplitude gradients. This is in some tension with the action of the momentum operator $\hat{p} = -i\hbar\nabla$, which creates terms proportional to $\nabla n(\mathbf{x}, t)$. The latter raises questions about the physical significance of eq. (1) in certain situations and in particular motivates a more detailed investigation of particle velocities in cases where density gradients in the wave function cannot be neglected. Such an investigation gains additional relevance due to the fact that eq. (1) finds applications in other areas of quantum physics, for example, as the guiding equation in the de Broglie-Bohm interpretation of quantum mechanics [4–7].

In fact, wave functions with density gradients are ubiquitous in quantum mechanics. When particles encounter a reflective potential step, for example, the wave function decays rapidly with a characteristic decay length depending on the mismatch between kinetic and potential energy. This decay occurs *within* the high-potential region, which distinguishes the quantum mechanical mode of motion from the classical one. The qualitative difference arises from the fact that quantum mechanical wave functions can have domains of negative kinetic energy, which allow them to migrate to the high-potential region without violating energy conservation [8, 9]. Since a state of negative (local) kinetic energy has no obvious classical equivalent, the question naturally arises as to what kind of motion it represents. This question is related but not identical to the problem of tunneling times, which has

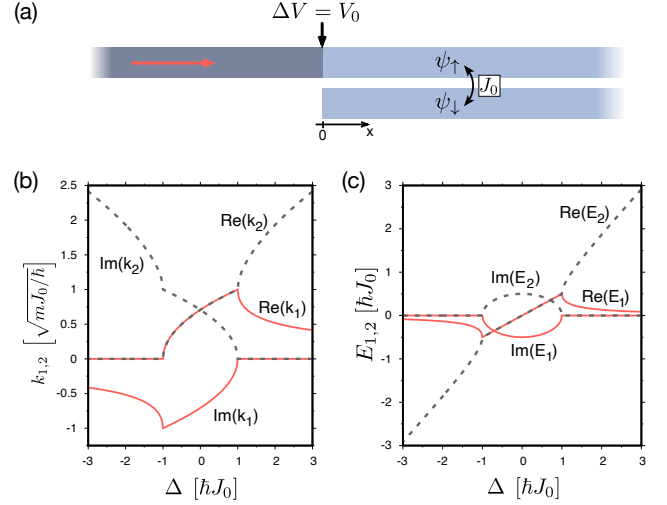


FIG. 1. (a) A stream of particles (red arrow) is transversally confined in a waveguide potential and propagates towards a potential step (vertical black arrow). At the step, a second waveguide opens up. The particle transfer between the upper and the lower waveguide, described by the coupling constant $J_0 > 0$, effectively acts as a clock allowing particle velocities to be determined by considering the population build-up in ψ_{\downarrow} . (b) Solution of the coupled Schrödinger eqs. (2) and (3) in terms of the real and imaginary parts of k_1 (solid red lines) and k_2 (dashed gray lines) as a function of $\Delta = E + \hbar J_0 - V_0$. (c) Real and imaginary part of $E_1 = (\hbar k_1)^2/2m$ (solid red lines) and $E_2 = (\hbar k_2)^2/2m$ (dashed gray lines).

existed since the dawn of quantum mechanics and has not been fully resolved to date, despite many advances. See Ref. [10–12] for overviews.

The study of velocities in quantum mechanics presents several difficulties. wave functions can contain superpositions of waves traveling in opposite directions. In such cases, velocity definitions that indicate a direction such as eq. (1) inevitably deliver different results than those that reflect the magnitude (absolute value) of the velocity of particles. Furthermore, the assignment of a *local* velocity to a wave function, as in eq. (1), to some extent goes beyond the conventional formalism of quantum mechanics that is mainly concerned with *global* quantities (i.e., eigen or expectation values with respect to the total wave function) [13]. In other words, the standard formalism of

* j.klaers@utwente.nl

quantum mechanics does not readily provide a method leading to the desired result. A well-known approach used in the tunneling time problem is the embedding of additional degrees of freedom in the system whose change can be interpreted as a time measurement (Larmor clock) [14–16]. Such an approach should be equally helpful in determining velocities.

In our work, we study the motion of massive particles in a system of two coupled waveguide potentials, where the population transfer between the waveguides effectively acts as a clock and allows particle velocities to be determined. In preparation, consider a time-dependent quantum mechanical system in which two (degenerate) states are coupled to each other with the coupling constant $J_0 > 0$. If the probability amplitude is initially entirely concentrated in one of the states, it is well known that the population in the initially unoccupied state follows $\sin^2(J_0 t)$ as a function of time t and, consequently, for small times increases like $(J_0 t)^2$. If we translate this time-dependent behavior into a propagating geometry (e.g., particles moving in coupled waveguides), we expect the spatial distribution of the population to be described by $\sin^2(J_0 x/v)$ with a velocity v . For small distances x , this can be approximated by $(J_0 x/v)^2$. Thus, provided that the coupling constant J_0 is known, one can infer the velocity by measuring the spatial population build-up in the initially unoccupied state. We consider the so-defined velocity to be a *particle* velocity (as opposed to a phase velocity) in the sense that its definition relies on actual population transfer between different parts of the system.

More specifically, we consider a system where a stream of particles with mass m is transversally confined in a waveguide potential and propagates towards a potential step at $x = 0$ with $V(x) = 0$ for $x < 0$ and $V(x) = V_0$ for $x \geq 0$. At the position of the potential step, another waveguide potential opens up, which runs parallel to the first one, see Fig. 1a. It is assumed that the potential barrier between both waveguides is small enough that coupling between the wave functions in the upper (ψ_\uparrow) and lower (ψ_\downarrow) waveguide takes place and is quantitatively described by the coupling constant $J_0 > 0$. For $x \geq 0$, the steady state of the system is described by the coupled time-independent Schrödinger equations

$$E\psi_\uparrow = -\frac{\hbar^2}{2m} \frac{\partial^2 \psi_\uparrow}{\partial x^2} + V_0 \psi_\uparrow + \hbar J_0 (\psi_\downarrow - \psi_\uparrow) \quad (2)$$

$$E\psi_\downarrow = -\frac{\hbar^2}{2m} \frac{\partial^2 \psi_\downarrow}{\partial x^2} + V_0 \psi_\downarrow + \hbar J_0 (\psi_\uparrow - \psi_\downarrow) . \quad (3)$$

The total energy $E > 0$ corresponds to the kinetic energy of the particles before they hit the potential step. Furthermore, we define the energy mismatch $\Delta = E + \hbar J_0 - V_0$.

For $E \gg V_0$, classical propagation beyond the potential step at $x = 0$ is possible and one expects that the wave functions in both waveguides can be represented by propagating plane waves whose amplitudes are harmonically modulated due to the waveguide coupling. A suitable ansatz to solving eqs. (2) and (3) is therefore

$\psi_\uparrow \propto \cos(k_1 x) \exp(ik_2 x)$ and $\psi_\downarrow \propto \sin(k_1 x) \exp(ik_2 x)$. Note that the relative population of the waveguides $p_i = |\psi_i|^2 / (|\psi_\uparrow|^2 + |\psi_\downarrow|^2)$ with $i = \uparrow, \downarrow$ depends exclusively on the population transfer factors $\cos(k_1 x)$ and $\sin(k_1 x)$. It turns out that this ansatz works not only for $E \gg V_0$ but also for arbitrary energies. This general solution is uniquely determined by setting several requirements, which includes the assumption of an incoming wave with unity amplitude, the continuity of the wave functions $\psi_{\uparrow, \downarrow}$ and their derivatives $\partial_x \psi_{\uparrow, \downarrow}$, and the requirement that $\text{Re}(k_2)$ [$\text{Im}(k_2)$] is a positive, continuous, and monotonically increasing [decreasing] function of Δ , as this reflects the expected behavior for $E \gg V_0$ [$E \ll V_0$]. With these requirements, the solution is

$$\psi_\uparrow = \frac{2k_0}{k_0 + k_2} \cos(k_1 x) e^{ik_2 x} \quad (4)$$

$$\psi_\downarrow = -\frac{2ik_0}{k_0 + k_2} \sin(k_1 x) e^{ik_2 x} , \quad (5)$$

with wavenumbers $k_{0,1,2}$ given by

$$k_0 = \sqrt{2mE/\hbar} \quad (6)$$

$$k_1 = mJ_0/\hbar k_2 \quad (7)$$

$$k_2 = \hbar^{-1} \sqrt{m \left(\Delta \pm \sqrt{\Delta^2 - (\hbar J_0)^2} \right)} , \quad (8)$$

where the '+' solution applies for $\Delta/\hbar J_0 > -1$ and the '-' solution otherwise. A graphical representation of this is shown in Fig. 1b and reveals three different regimes of propagation. For $\Delta/\hbar J_0 > 1$, k_2 is real-valued indicating classical propagation. For $\Delta/\hbar J_0 < -1$, k_2 is imaginary indicating exponential decay of the wave function. For $|\Delta|/\hbar J_0 \leq 1$, $k_{1,2}$ are complex conjugated to each other. In all three cases, the total energy is given by

$$E = \frac{(\hbar k_1)^2}{2m} + \frac{(\hbar k_2)^2}{2m} - \hbar J_0 + V_0 . \quad (9)$$

To begin the discussion of particle velocities, consider the limit $\Delta/\hbar J_0 \rightarrow \infty$, which describes large excess of kinetic energy with respect to the energy scale of the coupling. In this case, Fig. 1c suggests that the energy associated with the population transfer between the waveguides $E_1 = (\hbar k_1)^2/2m$ is negligible compared to Δ . Accordingly, we expect that the energy-velocity relation of the particles within a waveguide is not affected by the presence of the neighboring waveguide and should be simply given by $v = \sqrt{2\Delta}/m$. There are two ways to recover this velocity from the solution of the coupled Schrödinger equations. On the one hand, the plane wave factor $e^{ik_2 x}$ in the wave functions with $k_2 > 0$ allows a direct assignment of a (group) velocity of $v = \hbar k_2/m$. With $k_2 = \sqrt{2m\Delta}/\hbar$ following from eq. (8) in the limit $\Delta/\hbar J_0 \rightarrow \infty$, this gives the expected result for v . On the other hand, the population transfer factors $\cos(k_1 x)$ and $\sin(k_1 x)$ in the wave functions define a velocity via $k_1 x = J_0 x/v$, or $v = J_0/k_1$, associated with the idea that the higher the velocity of the particles, the further away

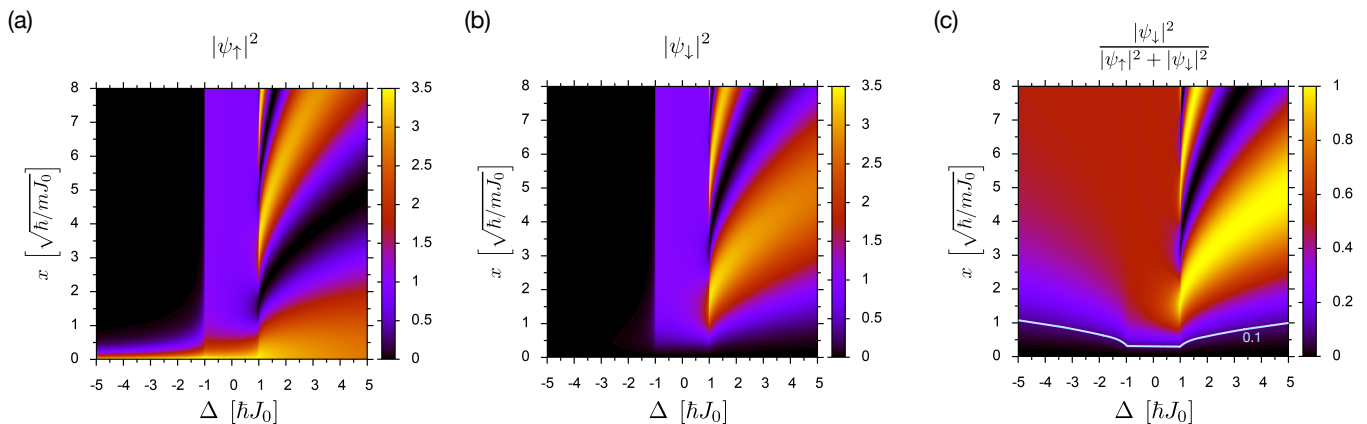


FIG. 2. Particle densities $|\psi_{\uparrow,\downarrow}|^2$ as a function of energy mismatch Δ and position $x > 0$ in the (a) upper and (b) lower waveguide. (c) Relative population in the lower waveguide $p_{\downarrow} = |\psi_{\downarrow}|^2 / (|\psi_{\uparrow}|^2 + |\psi_{\downarrow}|^2)$. Sufficiently close to the potential step ($x = 0$), both the classically allowed and the classically forbidden sides show the same relative population dynamics. The solid white line indicates a relative population of $p_{\downarrow} = 0.1$.

from the potential step the population build-up in the lower waveguide occurs. With $k_1 = \sqrt{m/2\Delta} J_0$ following from eq. (7) in the aforementioned limit, we equally recover $v = \sqrt{2\Delta/m}$. We note that the velocity determined in this way only reflects the magnitude of a velocity, since the population transfer between the waveguides does not define a direction of motion. This can only be determined from the further physical context.

Now consider a strongly negative energy mismatch $\Delta/\hbar J_0 \rightarrow -\infty$. Also in this limit $E_1 \ll \Delta$ holds, see Fig. 1c, and we do not expect the energy-velocity relation of the particles to be altered by the presence of the second waveguide. Since k_2 is purely imaginary, the plane wave factor $e^{ik_2 x} = e^{-|k_2|x}$ now describes an exponential decay, which does not provide a physically obvious interpretation in terms of a velocity. However, the latter does not apply to the population transfer factors. For $\Delta/\hbar J_0 \rightarrow -\infty$, we find $k_1 = \sqrt{m/2\Delta} J_0$ just as before. However, this time we have $\Delta < 0$, so that $k_1 = \sqrt{m/2|\Delta|} i J_0$ becomes imaginary. Physically, this means that the coupling of the waveguides effectively switches from dispersive ($J_0 > 0$) to dissipative (iJ_0) with the magnitude of the coupling remaining constant. In other words, the particle exchange between the waveguides is no longer particle number-conserving. As a result of this effectively dissipative coupling, the oscillating exchange of populations between the waveguides is replaced by a relaxation to equal occupation for $x \rightarrow \infty$, which can be seen from

$$p_{\downarrow} = \frac{\sinh^2(|k_1|x)}{\cosh^2(|k_1|x) + \sinh^2(|k_1|x)} \stackrel{x \rightarrow \infty}{\approx} \frac{1}{2}. \quad (10)$$

The population transfer dynamics, however, still suggests the presence of a well-defined velocity via $|k_1|x = J_0 x/v$, or $v = J_0/|k_1|$, with the same physical interpretation as before: the higher the velocity of the particles, the further away from the potential step the population build-

up in the lower waveguide occurs. This gives a clear physical meaning to the notion of a velocity for classically forbidden motion. Evaluating this expression, we obtain $v = \sqrt{2|\Delta|/m}$, which in this form covers both the classically allowed and classically forbidden case, as long as $|\Delta|/\hbar J_0 \rightarrow \infty$. We consider particles following this energy-velocity relation to be the most natural explanation to account for the fact that the population build-up in the lower waveguide depends on the energy of the incident particles - even in the classically forbidden case. We furthermore note that this expression for the velocity has been derived before, for example, using a WKB approximation [17] and is formally related to the Büttiker-Landauer time, which occurs in the discussion of tunneling times at potential barriers (of finite width) [18, 19].

We now consider the full solution of the model, which is represented in Fig. 2. Figures 2a,b show the population in the upper and lower waveguides for different energies Δ and positions $x > 0$. The relative population in the lower waveguide p_{\downarrow} is shown in Fig. 2c and generally indicates an oscillatory population transfer for positive and relaxation to equal populations for negative energy mismatch, which was already discussed in the limit $|\Delta|/\hbar J_0 \rightarrow \infty$. In the region $x/x_0 \lesssim 1$ with $x_0 = \sqrt{\hbar/mJ_0}$, however, the occupation of the lower waveguide p_{\downarrow} is observed to become a mirror-symmetric function of the energy mismatch Δ . This means that near the potential step, both the classically allowed and the classically forbidden sides show the same relative population dynamics. We now interpret this result with regard to particle velocities. Close to the potential step, a leading order approximation of the relative population build-up in the lower waveguide gives $p_{\downarrow} \simeq (|k_1|x)^2$ for all Δ . A comparison with $p_{\downarrow} \simeq (J_0 x/v)^2$ suggests $v = J_0/|k_1|$, or

$$v_J = \sqrt{\frac{|\Delta \pm \sqrt{\Delta^2 - (\hbar J_0)^2}|}{m}}, \quad (11)$$

where the '+' solution applies for $\Delta/\hbar J_0 > -1$ and the '-' solution otherwise. The obtained velocity as a function of Δ is graphically represented in Fig. 3a. In particular, v_J is observed to be mirror-symmetric with respect to $\Delta = 0$ and constant in the range $|\Delta|/\hbar J_0 \leq 1$. For comparison we consider the phase gradient velocity v_S following from eq. (1), which is equivalently given by $v_S = j/|\psi|^2$ with the probability current $j = \hbar(\psi^* \partial_x \psi - \text{h.c.})/2im$. $v_S(0)$ vanishes for $\Delta/\hbar J_0 \leq -1$. However, as is demonstrated by the inter-waveguide population dynamics this should not be understood as absence of motion. As further comparison in Fig. 3a, we consider the velocity v_p derived from the local momentum associated with a wave function ψ following $v_p = |\psi|^{-1} \hat{p} \psi / m$. Evaluating v_p for ψ_\uparrow at $x = 0$ indeed recovers the velocity derived from the population transfer, see Fig. 3a. Similar to v_J and evident from its definition, $v_p(0)$ reflects the magnitude of a velocity but indicates no direction.

In the remainder of this work, we will discuss the properties of the model in the region $|\Delta|/\hbar J_0 < 1$ in more detail. First, we will argue that the motional states in this region are classically forbidden. An argument supporting this claim derives from the behavior of the (local) kinetic energy T , which is fed both by the motion along the waveguides and by the motion (hopping) between the waveguides, and accordingly is given by the first three terms in eq. (9): $T = E_1 + E_2 - \hbar J_0$. Based on Fig. 1c, T changes sign at $\Delta/\hbar J_0 = 1$ or equivalently $E = V_0$ [because of $\text{Re}(E_{1,2}) = \hbar J_0/2$ and $\text{Im}(E_1) = -\text{Im}(E_2)$] and remains negative for all $\Delta < \hbar J_0$. As discussed in the introduction, a negative (local) kinetic energy has no classical analogue and can therefore serve as an indicator showing the transition between classically allowed and classically forbidden behavior. This argument, together with the fact that the wave function extends macroscopically beyond the potential step, see Fig. 2a,b, shows that our model for $|\Delta|/\hbar J_0 < 1$, which we now call the transparency region, describes long-range particle transport in a classically forbidden regime.

We will examine the transport properties in the transparency region in more detail. Because $E_{1,2}$ and Δ are all of the same order of magnitude now, see Fig. 1c, the state in the lower waveguide can have a significant impact on the motion in the upper one and vice versa. The velocity at the potential step, see eq. (11), is therefore to be interpreted as a local velocity, which will change for $x > 0$ with the changing relative populations in the waveguides (despite constant potential energy). To find out the characteristics of long-range transport, it is thus necessary to obtain the mean or asymptotic particle velocities. In the transparency region, we have $\text{Re}(k_1) = \text{Re}(k_2)$ and $\text{Im}(k_1) = -\text{Im}(k_2)$, see Fig. 1b. For $x \gg x_0$, the wave functions in eqs. (4) and (5) then asymptotically approach $\psi_{\uparrow,\downarrow} \propto \exp(i2\text{Re}(k_2)x)$ associated with a frequency $\omega = \hbar(2\text{Re}(k_2))^2/2m$. Thus, the states reduce to standard plane waves with a single real wavenumber $k' = 2\text{Re}(k_2)$, which allows the usual definitions of phase and group velocities to be applied in this situation.

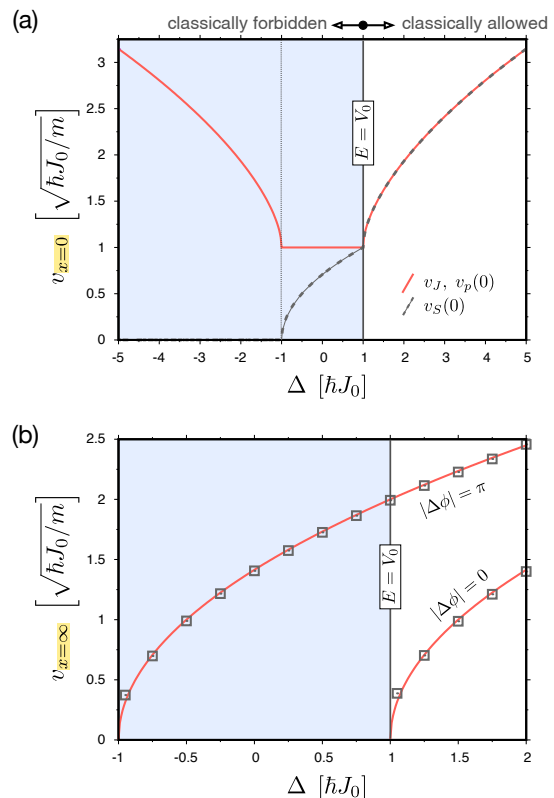


FIG. 3. (a) Particle velocity at the potential step. The velocity v_J [solid red line] is derived from the population transfer between the waveguides following eq. (11). The velocity $v_p(0)$ [also solid red line] is derived from the local momentum associated with the wave function ψ_\uparrow at $x = 0$, as defined in the main text. The velocity $v_S(0)$ [dashed gray line] follows from eq. (1) and vanishes for $\Delta/\hbar J_0 \leq -1$. (b) Asymptotic velocities far from the potential step. In the transparency region, this is given by $v_\infty = \hbar 2\text{Re}(k_2)/m$. In the classically allowed region, in-phase (denoted by $|\Delta\phi| = 0$) and anti-phase ($|\Delta\phi| = \pi$) modes of propagation are possible (with $\Delta\phi = \arg \psi_\uparrow - \arg \psi_\downarrow$). These correspond to group velocities of $v_\infty = \hbar(k_2 \pm k_1)/m$. The data points (squares) follow from numerically integrating the time-dependent coupled Schrödinger equations associated with eqs. (2) and (3), assuming narrow-bandwidth Gaussian wave packets moving towards the potential step with varying (kinetic) energies as starting conditions. The Gaussian wave packets are created around a central position of $x = -2.5$ mm with a spatial extension of $\sigma = 0.4$ mm (standard deviation). Their velocity is determined by following the wave packet density maximum as a function of time. The numerical integration is performed using the 4th-order Runge-Kutta method with adaptive time steps. We assume $J_0 = 2\pi \cdot 20$ GHz and $m = 6.5 \cdot 10^{-36}$ kg.

With this, we immediately see that phase and group velocities are given by $v_{\text{ph},\infty} = \omega/k' = \hbar\text{Re}(k_2)/m$ and $v_\infty = \partial\omega/\partial k' = \hbar 2\text{Re}(k_2)/m$ with $v_\infty/v_{\text{ph},\infty} = 2$, which is the expected ratio for a free massive particle. Figure 3b shows v_∞ as a function of Δ in the transparency region and in the adjoining classically allowed region. In the latter, two distinct modes of propagation exist, which are

described by wave functions $\psi_{\uparrow,\downarrow} \propto e^{i(k_2 \pm k_1)x}$ and lead to different group velocities $v_{\infty} = \hbar(k_2 \pm k_1)/m$. These modes differ in the phase relation between ψ_{\uparrow} and ψ_{\downarrow} , see the caption of Fig. 3 for further details. We note that both modes merge for $\Delta/\hbar J_0 \rightarrow \infty$. In addition to the analytic solution, Fig. 3b includes supporting results from numerically integrating the time-dependent coupled Schrödinger equations associated with eqs. (2), (3), assuming Gaussian wave packets with varying energies as starting conditions, see caption of Fig. 3 for further details. In the classically allowed region, these simulations show the splitting of the incoming wave packet into two wave packets propagating at different velocities.

In this work, we argue that density gradients in wave functions are indicative of a genuine quantum mechanical type of motion, which associates wave function decay with a well-defined particle velocity that can be made visible in a system of coupled waveguides. In particular, our analysis suggests an energy-velocity relation of $v = \sqrt{2|\Delta|/m}$ in regions of exponentially decaying wave functions and the existence of classically forbidden long-range particle transport. This mode of transportation

effectively acts as a beamsplitter dividing the incoming particle stream into two equally strong parts. The splitting mechanism does not depend on material parameters and, within the bandwidth of the coupling, is independent of the energy of the incident particles. We expect that an experimental demonstration of the predicted effects is within reach, particularly in two-dimensional photon or exciton-polariton gases [20], where precise control of the potential landscape [21–23] and full experimental access to the wave function are possible.

ACKNOWLEDGMENTS

We thank Charlie Mattschas and Marius Puplauskis for carefully proofreading the manuscript and useful discussions. This work has received funding from the European Research Council (ERC) under the European Union’s Horizon 2020 research and innovation programme (Grant Agreement No. 101001512) and from the NWO (grant no. OCENW.KLEIN.453).

-
- [1] L. Landau, Theory of the superfluidity of helium II, *Phys. Rev.* **60**, 356 (1941).
 - [2] P. W. Anderson, Considerations on the flow of superfluid helium, *Rev. Mod. Phys.* **38**, 298 (1966).
 - [3] A. J. Leggett, Superfluidity, *Rev. Mod. Phys.* **71**, S318 (1999).
 - [4] D. Bohm, A suggested interpretation of the quantum theory in terms of "hidden" variables. I, *Phys. Rev.* **85**, 166 (1952).
 - [5] P. R. Holland, *The quantum theory of motion: an account of the de Broglie-Bohm causal interpretation of quantum mechanics* (Cambridge university press, 1995).
 - [6] J. O. Hirschfelder, A. C. Christoph, and W. E. Palke, Quantum mechanical streamlines. I. Square potential barrier, *J. Chem. Phys.* **61**, 5435 (1974).
 - [7] D. Bohm and B. J. Hiley, Non-locality and locality in the stochastic interpretation of quantum mechanics, *Phys. Rep.* **172**, 93 (1989).
 - [8] Y. Aharonov, S. Popescu, D. Rohrlich, and L. Vaidman, Measurement of the negative kinetic energy of tunneling particles, in *Proc. 4th Int. Symp. Foundations of Quantum Mechanics, Tokyo* (1992).
 - [9] Y. Aharonov, S. Popescu, D. Rohrlich, and L. Vaidman, Measurements, errors, and negative kinetic energy, *Phys. Rev. A* **48**, 4084 (1993).
 - [10] E. Hauge and J. Støvneng, Tunneling times: a critical review, *Rev. Mod. Phys.* **61**, 917 (1989).
 - [11] R. Landauer and T. Martin, Barrier interaction time in tunneling, *Rev. Mod. Phys.* **66**, 217 (1994).
 - [12] U. S. Sainadh, R. T. Sang, and I. V. Litvinyuk, Attoclock and the quest for tunnelling time in strong-field physics, *J. Phys. Photonics* **2**, 042002 (2020).
 - [13] This is related to the topic of 'weak values', see: Y. Aharonov and L. Vaidman, Properties of a quantum system during the time interval between two measurements, *Phys. Rev. A* **41**, 11 (1990).
 - [14] A. Baz, Lifetime of intermediate states, *Yad. Fiz.* **4**, 252 (1966).
 - [15] V. Rybachenko, Time of penetration of a particle through a potential barrier, *Yad. Fiz.* **5**, 895 (1967).
 - [16] R. Ramos, D. Spierings, I. Racicot, and A. M. Steinberg, Measurement of the time spent by a tunnelling atom within the barrier region, *Nature* **583**, 529 (2020).
 - [17] A. Jayannavar, A note on traversal time for tunneling, *Pramana* **29**, 341 (1987).
 - [18] M. Büttiker and R. Landauer, Traversal time for tunneling, *PRL* **49**, 1739 (1982).
 - [19] M. Büttiker, Larmor precession and the traversal time for tunneling, *Phys. Rev. B* **27**, 6178 (1983).
 - [20] J. Bloch, I. Carusotto, and M. Wouters, Non-equilibrium Bose-Einstein condensation in photonic systems, *Nat. Rev. Phys.* **4**, 470 (2022).
 - [21] C. Kurtscheid, D. Dung, A. Redmann, E. Busley, J. Klaers, F. Vewinger, J. Schmitt, and M. Weitz, Realizing arbitrary trapping potentials for light via direct laser writing of mirror surface profiles, *EPL* **130**, 54001 (2020).
 - [22] M. Vretenar, B. Kassenberg, S. Bissesar, C. Toebes, and J. Klaers, Controllable Josephson junction for photon Bose-Einstein condensates, *Phys. Rev. Res.* **3**, 023167 (2021).
 - [23] M. Vretenar and J. Klaers, Mirror surface nanostructuring via laser direct writing—Characterization and physical origins, arXiv preprint arXiv:2211.05096 (2022).